Ferrofluid rotary seal with replenishment system for sealing liquids

van der Wal, Karoen; van Ostayen, Ron A.J.; Lampaert, Stefan G.E.

DOI
10.1016/j.triboint.2020.106372

Publication date
2020

Document Version
Final published version

Published in
Tribology International

Tribology International 150 (2020) 106372

Contents lists available at ScienceDirect

Tribology International

journal homepage: http://www.elsevier.com/locate/triboint

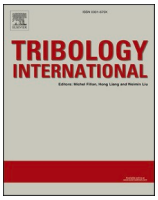

Ferrofluid rotary seal with replenishment system for sealing liquids

Karoen van der Wal, Ron A.J. van Ostayen, Stefan G.E. Lampaert *

Department of Precision and Microsystems Engineering, Delft University of Technology, Mekelweg 2, 2628 CD, Delft, the Netherlands

ARTICLE INFO

Keywords:
Magnetic liquid seal
Lip seal
Water
Ferrofluid transport
Magnetics

ABSTRACT

Ferrofluid rotary seals are mechanical contact-free magnetic liquid seals that are characterised by their simple structure, low friction and ability to hermetically seal. Although ferrofluid rotary seals for sealing vacuum and gases are part of a well established industry, the sealing of liquids has not been implemented yet. Literature learns that degradation of the ferrofluid seal over time when it dynamically contacts a liquid results into premature seal failure. This paper presents a new type of ferrofluid rotary seal in which a ferrofluid replenishment system is implemented that renews the ferrofluid in the sealing ring while sealing capacity is maintained. By replacing the degraded ferrofluid in the seal at a sufficient rate, service life of the ferrofluid rotary seal can theoretically be unlimited. An analytical model and FEM analysis are used to design the ferrofluid sealing device and to predict its sealing capacity. An experimental test setup has been built on which the sealing capacity and service life of the device has been tested for different sealing conditions. It is demonstrated that the ferrofluid replenishment system successfully extends and controls the service life of the ferrofluid rotary seal that dynamically seals pressurised water.

1. Introduction

In the 1960's the world's first patented magnetic fluid was created by adding magnetic properties to rocket fuel, enabling control of the fluid in outer space using magnets [1]. Funded by space agency NASA Ronald E. Rosensweig led the development of a wide variety of magnetic fluids and the research to the fluid mechanics of magnetic liquids [2,3]. Ferrofluid is a magnetic fluid that consists of ferromagnetic nanoparticles suspended in a carrier liquid [4]. The three main technical application areas of ferrofluids are sealing, damping and heat transfer [5]. In most of these applications ferrofluid is positioned magnetically and secondary properties of the fluid are then exploited. An example of application are ferrofluid planar bearings, where absence of both stick slip and mechanical contact result in respectively a high precision and high durability [6,7].

Since the 1930's radial lip seals are industries standard to retain lubricant and exclude contamination in rotating shaft and bearing applications [8]. This contact-based rotary seal is inherently subjected to wear, which limits its service life and causes leaks. Ferrofluid rotary seals are contact-free magnetic liquid seals and are characterised by their simple structure, low friction and ability to hermetically seal. Ferrofluid rotary seals operating in vacuum and gas environments already have proven themselves in industry [9–11]. Ferrofluid sealing is also considered to be very important in preserving the environment, since ferrofluid is able to create hermetic sealing for hazardous gases [12].

However, literature learns that ferrofluid rotary seals fail prematurely when they are used for sealing liquids [13–17]. The driving mechanisms causing this premature failure are not fully understood and prevent current implementation for sealing liquids. Many authors attribute this limited service life to the arise of interfacial instabilities between the liquid that is sealed and the ferrofluid of the seal [13,18]. When the liquid-ferrofluid interface becomes unstable, ferrofluid emulsifies with the liquid sealed which results in failure of the seal. Mitamura et al. have shown that a shielding structure in front of the ferrofluid rotary seal can be used to stabilise the interface between the two fluids [19–21]. Although shielding prevents instant seal failure caused by interfacial instability, the service life of the seal is still limited and unpredictable.

It is reported in literature that the magnetic properties of ferrofluid in contact with water decrease [22]. Also it is suggested that the existence of shearing forces at the interface of the ferrofluid seal and liquid contained limits its service life [23]. Shear forces between the liquid sealed and ferrofluid could cause gradual removal of ferrofluid [24]. All these effects could attribute to the degradation of the ferrofluid seal when it seals a liquid in dynamic operation conditions. Degradation decreases

* Corresponding author.
E-mail address: s.g.e.lampaert@tudelft.nl (S.G.E. Lampaert).

https://doi.org/10.1016/j.triboint.2020.106372
Received 24 December 2019; Received in revised form 22 March 2020; Accepted 10 April 2020
Available online 7 May 2020

the sealing capacity of the seal over time and causes seal failure when its sealing capacity becomes lower than the required operational sealing pressure.

If the service life can be improved ferrofluid sealing technology seems very promising for marine applications such as the sealing of propeller shafts of boats [25,26]. Also in medical applications the sealing technology seems to be very interesting. A lot of research is done to the ferrofluid sealing of blood in rotary blood pumps [27].

This paper presents a new type of ferrofluid rotary seal in which a ferrofluid replenishment system is implemented that renews the ferrofluid in the sealing ring while sealing capacity is maintained. By replacing the degraded ferrofluid in the seal at a sufficient rate, service life of the ferrofluid rotary seal that seals liquids can theoretically be unlimited. First an analytical model and FEM analysis of the ferrofluid sealing device is presented. Next the stability of the ferrofluid in the seal, the shielding and the ferrofluid replenishment method is discussed. The acquired knowledge is used to design an experimental test setup for a series of experiments in order to identify both static and dynamic sealing capacity of the system. Finally these results are used to perform a series of experiments in order to validate the hypothesis that the ferrofluid replenishment system improves the service life of the ferrofluid rotary seal that is used to seal high pressure water on a rotating shaft.

2. Methods

In order to design a ferrofluid rotary seal that seals liquids, first an analytical model that describes its sealing capacity is derived. Subsequently the required magnetic field intensities for this analytical model are calculated by FEM analysis performed using COMSOL Multiphysics©. Next, the influence of the magnetic field gradient stability of ferrofluid on its sealing capacity is discussed. In order to prevent dynamic seal failure, shielding of the seal is discussed and the new concept of ferrofluid replenishment is introduced. Finally, the experimental test setup and experimental procedures and results are elaborated.

2.1. Analytical model

A cross-sectional overview of a basic ferrofluid rotary sealing system is presented in Fig. 1. The system consists of an axially magnetised ring magnet that is placed around a ferromagnetic shaft and supported by a non magnetic structure (green). Two ferrofluid seals that are located in the gap between the rotating shaft and stationary housing maintain the pressure difference between the liquid with pressure p_l that is sealed and the atmosphere with pressure p_0. In order to calculate the static sealing capacity of the two ferrofluid seals in the sealing system an analytical

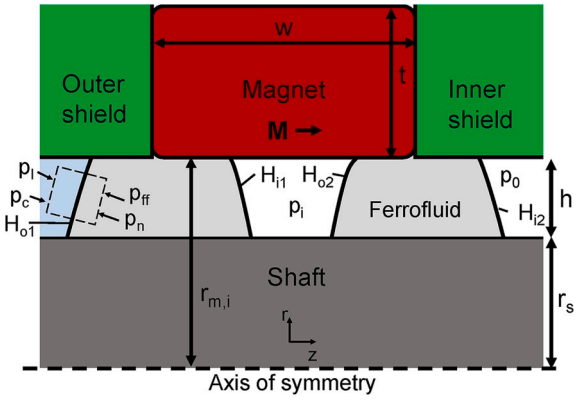

Fig. 1. Cross-sectional overview of the ferrofluid rotary sealing system that consists of an axially magnetised ring magnet surrounding a ferromagnetic shaft. Ferrofluid magnetically positioned in the seal gap prevents liquid to leak through the seal gap. The inner and outer shield are made of non-ferromagnetic material.

model is derived. The behaviour of the ferrofluid in terms of its motion as a function of time can be described using the Navier-Stokes equations for Newtonian incompressible magnetic fluids [28], presented in relation 1.

$$\rho_{ff}\frac{\mathrm{D}\mathbf{v}}{\mathrm{D}t} = \underbrace{-\nabla p_{ff}}_{\text{Pressure}} + \underbrace{\eta\nabla^2\mathbf{v}}_{\text{Viscous}} + \underbrace{\rho_{ff}\mathbf{g}}_{\text{Gravity}} + \underbrace{\mu_0 M\nabla H}_{\text{Magnetic}} \qquad (1)$$

$$\nabla\cdot\mathbf{v} = 0$$

The left side term is the density of the ferrofluid ρ_{ff} times the rate of change following the mass motion $\mathbf{v}$, also known as the material derivative. The right side of equation (1) is the sum of the pressure, viscous, gravity and magnetic body forces normalised to a unit volume. In general gravitational effects are small and can be neglected. For the derivation of the analytical model only non-rotating static shaft conditions are considered, which means that inertial and viscous effects on the pressure distribution can be neglected. The relation presented in equation (1) can now be reduced to the relation shown in equation (2) and only contains the pressure and magnetic terms.

$$\nabla p_{ff} = \mu_0 M\nabla H \qquad (2)$$

where p_{ff} is the pressure inside of the ferrofluid, μ_o the permeability of vacuum, M magnetisation of the ferrofluid and H the magnetic field intensity. The sealing capacity of a ferrofluid seal is defined to be the maximum pressure difference between the high pressure of the fluid (p_{ff}) and the low pressure (p_0) of the ambient gas that can be maintained without leakage. In order to calculate the sealing capacity of both ferrofluid seals combined ($p_l - p_0$), the boundary conditions at the interfaces of the seals have to be investigated. In Fig. 1 the dashed box indicates the boundary condition at the interface between the liquid that is sealed and the ferrofluid of the first seal. Equation (3) presents this boundary condition.

$$p_l + p_c = p_{ff} + p_n \qquad (3)$$

Besides bulk pressures p_l and p_{ff} also interfacial pressures p_n and p_c are present at the liquid-ferrofluid interface. Pressure p_c is the capillary pressure between the liquid that is contained and the ferrofluid and pressure p_n is the normal magnetic pressure. Capillary pressures will be neglected in the analytical model of the sealing capacity, considering its impact is low compared to the magnetic pressures generated inside of the ferrofluid [29]. The magnetic normal pressure p_n is equal to $\mu_0 M_n^2/2$, where M_n is the normal magnetisation force vector at the interface of the ferrofluid seal. The normal magnetic pressure p_n for the ferrofluid seals can also be neglected since the magnetic field is tangential to the interfaces of the ferrofluid seal [28]. At the three other interfaces of the sealing system also the normal magnetic pressure and the capillary pressure will be neglected.

With these assumptions the pressure build up in the first seal can be calculated using equation (2). The magnetisation M of the ferrofluid is a function of the magnetic field intensity. Since the magnetic field intensity in the sealing gap is high compared to the saturation magnetisation (M_s) of ferrofluid, it is safe to assume thatthe ferrofluid will be fully magnetically saturated ($M = M_s$). The maximum pressure difference between p_l and p_i then can be calculated by integrating in axial direction along the length of the seal, which is presented in equation (4).

$$p_l - p_i = \int_c \nabla p_{ff}\cdot\mathrm{d}\mathbf{z} = \mu_0 M_s\int_c \nabla H\cdot\mathrm{d}\mathbf{z}$$
$$= \mu_0 M_s(H_{o1} - H_{i1}) \qquad (4)$$

Equation (4) learns that the pressure build up of the first seal depends on the magnetic field intensity H_{o1} at the liquid-ferrofluid interface and the magnetic field strength H_{i1} at the ferrofluid interface on the inside of the seal. The sealing capacity of the second seal can be calculated in a similar way, but now with the magnetic field strength H_{o2} at the

interface on the inside of the seal and the magnetic field strength H_{i2} at the ferrofluid-air interface. Relation 5 presents the calculation of the total pressure build up $p_l - p_0$ of both seals combined.

$$p_l - p_0 = \mu_0 M_s((H_{o1} - H_{i1}) + (H_{o2} - H_{i2})) \quad (5)$$

When pressure difference $p_l - p_0$ on the two ferrofluid seals exceeds the sealing capacity of the two seals that is predicted by relation 5, the seals will burst and the liquid that is sealed will leak through the seal gap.

2.2. FEM analysis

Equation (5) presented in section 2.1 learns that the magnetic field intensities ($H_{o1}, H_{i1}, H_{o2}, H_{i2}$) at the interfaces of the two ferrofluid seals are required in order to calculate its static sealing capacity. These magnetic field intensities are calculated using the numerical analysis package COMSOL Multiphysics version 5.3.

The magnetic properties of the shaft material have a significant impact on the distribution of the magnetic field intensity in the seal system. Shafts that operate in aqueous environments and transmit torque often are made of stainless steel. There are four main families of stainless steels which are primarily classified by their crystalline structure. These are ferritic, austenitic, martensitic and duplex stainless steels. Of these four ferritic stainless steels have the best magnetic properties. Therefore the material of the shaft is selected to be ferritic stainless steel (AINSI 430F) and is modelled using the BH curve from the COMSOL material library (stainless steel 430F annealed). The ring magnet is modelled by a remanent magnetisation $\mathbf{B}_r$ and is magnetised in axial direction. Fillets of radius r_{fil} of the used ring magnet are constructed in all corners. Seal gap h of the seal system is 100 μm. Table 1 presents an overview of the parameters of the ferrofluid sealing device that is used in the FEM analysis.

Fig. 2 presents a two dimensional plot of the magnetic field intensity in the system. The colour scale represents the strength of the magnetic field, where red is highest magnetic field intensity and white the lowest. The black lines in the seal gap represent the magnetic isolines. Equation (2) learns these isolines are equal to the isolines of the pressure distribution in the system. Ferrofluid shapes according to these isolines. Analysing the distribution and shape of these lines it can be observed that two independent ferrofluid seals can be formed by the magnetic field distribution in the seal.

The magnetic field distribution of the seal system is evaluated along two horizontal lines in the sealing gap, one at the top of the gap (h) and one at bottom. Fig. 3 presents a lineplot of these magnetic field intensities. Previous section showed that the sealing capacity of the ferrofluid seals depends on the magnetic field differences $H_{o1} - H_{i1}$ and $H_{o2} - H_{i2}$. Since the seal will start to fail at its weakest spot, the magnetic field intensities that predict the lowest sealing capacity have to be used.

In order to reach the full performance potential of the seal system the magnetic field difference ΔH on each ferrofluid seal has to be as high as possible. The inner shield, also shown in Fig. 1, makes sure that the ferrofluid of the second seal is forced into a region of low magnetic field intensity (H_{i2}). The magnetic field intensity plot of Fig. 3 learns that the inner shield has to have a width of around 6 mm in order to create a high magnetic field difference on the second seal and therefore a high sealing capacity.

Table 1
Parameters of the sealing system which are used in the FEM analysis.

Design Parameters			
r_{fil}	0.3 mm	$\mathbf{B}_r$	1.28 T
r_s	3.9 mm	w	6 mm
$r_{m,i}$	4 mm	h	100 μm
t	3.5 mm	M_s	35 kA/m

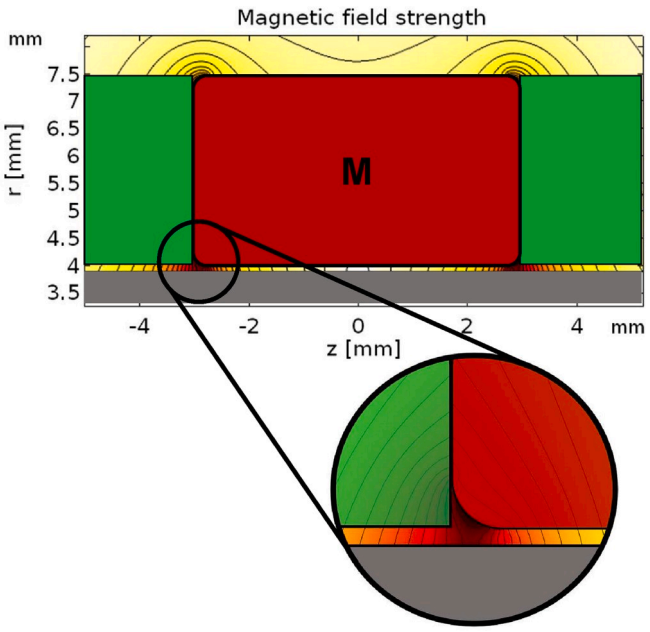

Fig. 2. Magnetic field intensity of the seal having a ferritic stainless steel (AINSI 430F) shaft. The isolines of the magnetic field intensity are also the isolines of the pressure distribution in the ferrofluid. Ferrofluid shapes according to these isolines.

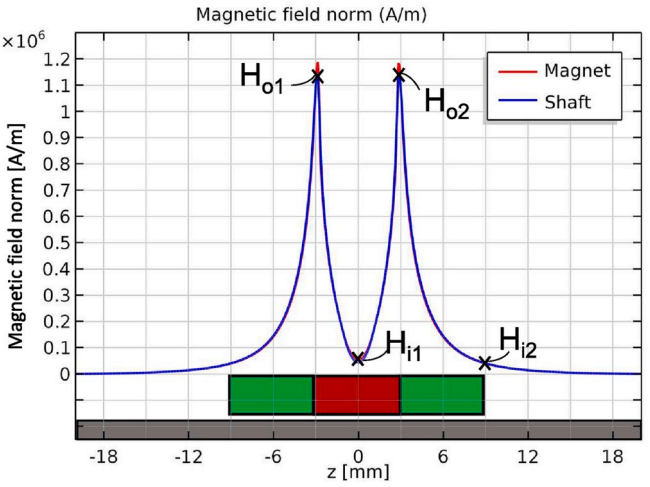

Fig. 3. Magnetic field intensity evaluated at two horizontal lines in axial direction at the top and bottom surfaces of the seal gap. The material of the shaft is ferritic stainless steel (AINSI 430F).

The ferrofluid (Ferrotec EFH1) that will be used in the experimental sealing system consists of a light hydrocarbon carrier liquid with magnetite (Fe_3O_4) suspended particles. The saturation magnetisation of the ferrofluid M_s equals 35 kA/m. Table 2 lists the magnetic field intensities at the two interfaces of both seals which have been found in the FEM analysis. The sealing capacity of both seals now can be calculated using equation (2). The total predicted sealing capacity of the two

Table 2
Magnetic field intensities at the seal interfaces and predicted sealing capacity of both ferrofluid seals.

	$H_o \cdot 10^5$ [A/m]	$H_i \cdot 10^5$ [A/m]	Δp [kPa]
Seal 1	11.4	0.541	47.8
Seal 2	11.4	0.410	48.4

ferrofluid seals combined equals 96.2 kPa.

2.3. Magnetic field gradient stability of ferrofluid

Since the ferrofluid in the sealing system is a colloidal dispersion of magnetic particles in a liquid carrier, stability of that colloid is an important property of the seal. In static sealing conditions the magnetic field gradient in the seal generated by the ring magnet, shown in Fig. 2, can cause migration of the magnetic particles. Particles travel through the fluid to a higher intensity region of the magnetic field [30]. This phenomenon results in a non homogeneous ferrofluid that has a higher effective magnetisation. The sealing capacity that is measured will be higher than predicted using relation 5. By rotating the shaft at sufficient speed the ferrofluid in the seal becomes homogeneous again.

The stability of the magnetic particles in the magnetic field gradient can be analysed by comparing their thermal energy E_{Therm} and magnetic energy E_{Mag}. Thermal motion counteracts the magnetic field force and provides statistical motion that results in a distribution of the particles in the magnetic fluid. In equation (6) the ratio between both energies is presented.

$$\frac{E_{Therm}}{E_{Mag}} = \frac{k_B T}{\mu_0 M_p H V_p} \tag{6}$$

The thermal energy per particle can be calculated by the product of the Boltzmann's constant k_B and absolute temperature T. The magnetic energy represents the work in transferring the particle to the higher magnetic intensity region in the fluid. The magnetic energy per particle E_{Mag} can be calculated by the product of magnetic permeability of vacuum μ_0, magnetisation of the particle M_p, magnetic field intensity H and particle volume V_p. It can be concluded that particle size, temperature of the ferrofluid in the seal gap and magnetisation of the particles are important factors that influence the stability of the ferrofluid in the magnetic field gradient that is present in the seal.

2.4. Shielding

A relative velocity between the liquid that is sealed and the ferrofluid of the seal can cause interfacial instability which results in seal failure [13,31]. By introducing a shield into the design of a ferrofluid seal sealing liquids the liquid-ferrofluid interface can be stabilised and instant seal failure due to interfacial instability can be prevented [19,21]. The simple outer shield structure presented in Fig. 1 is found to be most effective [19]. Experiments and CFD analyses of flow in a ferrofluid seal showed the shield stabilises the interface between water and the ferrofluid. Fig. 4 visualises the velocity profiles of the liquid sealed and the ferrofluid of the seal when a no slip condition is assumed. Also it is assumed flows in and in front of the seal gap are laminar and that the velocity profiles are linear in radial direction.

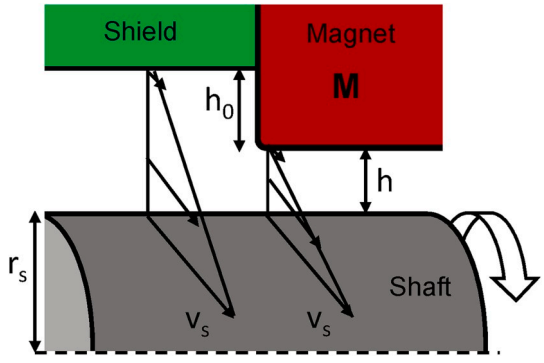

Fig. 4. Velocity profiles of the liquid that is sealed and the ferrofluid of the seal. Due to a height difference h_0 between the magnet and shield of the system a relative velocity between the fluids is created.

Equation (7) presents a relation for calculating the relative velocity between the liquid that is sealed and ferrofluid of the system.

$$v_{ff} - v_l = v_s \cdot \frac{h_0}{h_0 + h} \tag{7}$$

where v_{ff} and v_l are the velocities of ferrofluid and liquid that is sealed, v_s the surface speed of the shaft and h_0 the difference in gap height between the shield and seal gap h. If a seal system design is considered with a large ratio between h_0 and h, the velocity difference can be approximated by surface speed v_s. It can be seen that the height difference h_0 is an important design parameter for minimising relative velocity between the liquids and the prevention of premature seal failure.

The Kelvin-Helmholtz instability for magnetic liquids derived by Rosensweig is often used to describe the stability of the liquid-ferrofluid interface [13,18,28]. The Kelvin-Helmholtz instability is a hydrodynamic instability in which two inviscid fluids are in relative and irrotational motion. The velocity and density profiles are discontinuous at the interface between the two fluids. Besides preventing instability of the interface between the liquid sealed and ferrofluid, shielding also decreases shearing forces on the ferrofluid. Shearing stress on the ferrofluid is dependent on viscosity, the relative velocity of the fluids and the contact area between the liquids. When shaft diameter and seal gap of the system increases, shear stresses affecting the performance of the seal will also increase.

2.5. Ferrofluid replenishment system

Although shielding of a ferrofluid rotary seal that seals liquids prevents instant dynamic seal failure due to interfacial instability, service life of the seal is still limited. Degradation of the ferrofluid seal decreases the sealing capacity over time and causes failure of the seal when its sealing capacity becomes lower than the required operational sealing pressure.

In order to solve this problem, a ferrofluid replenishment system is introduced here into the design of a ferrofluid rotary seal (also partially presented in Ref. [32,33]). The system replenishes the ferrofluid of the seals by facilitating the axial transport of ferrofluid from one seal to another.

Fig. 5 presents an overview of the process of ferrofluid transport through the two seals of the ferrofluid rotary sealing system that also was elaborated in sections 2.1 and 2.2. First an amount of new ferrofluid is radially injected through a supply channel in front of the first seal (step 1). By doing so the same amount of ferrofluid at the lowest pressure region of the first seal (interface of H_{i1}) will jump from the first seal to

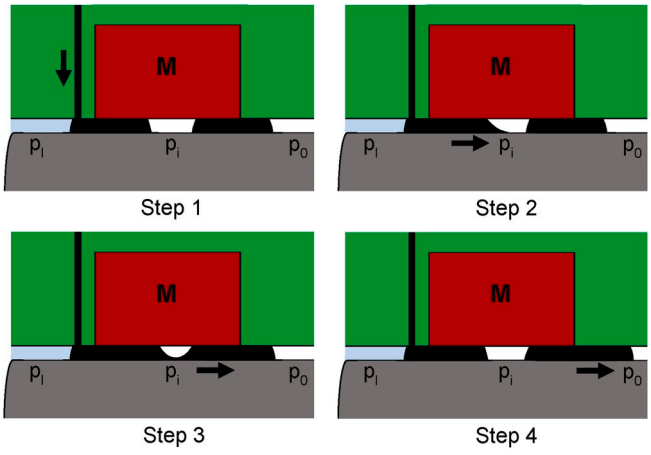

Fig. 5. Concept of the axial ferrofluid transport through the seal. During step 1 new ferrofluid is radially added in front of the first seal. In steps 2 and 3 ferrofluid flows from the first seal to the second seal. In step 4 ferrofluid of the second seal is pushed to the ferrofluid outlet at the right.

the second seal. This can be seen in steps 2 and 3 presented in Fig. 5. When the second seal is supplied with ferrofluid from the first seal, ferrofluid at the lowest pressure region of the second seal (interface of H_{i2}) will be pushed out of the seal to the right through the sealing channel (step 4). This ferrofluid will eventually be pushed to the end of the sealing channel where it can be collected, potentially for recycling.

The sealing capacity of the ferrofluid seals is restored when the degraded ferrofluid is replaced by new ferrofluid. If the ferrofluid in the seal constantly is being replaced at sufficient rate, the service life of the ferrofluid rotary seal theoretically could be extended without limitation.

In order to prevent the ferrofluid from flowing towards the liquid that is sealed instead of through the seals, it is required that the liquid pressure p_l is sufficiently high in order to force the ferrofluid to jump from the first to the second seal. In Fig. 3 the magnetic field intensity H_{i1} between the two seals can be seen. This magnetic field intensity can be used to calculate a pressure p_{min}, in order to define the operational range of the sealing system to use this axial ferrofluid transport. The sealing capacity of the seal system can be increased when multiple seals are placed after each other [34]. Equation (8) presents a general relation for the upper- and lower-bound of liquid pressure p_l for the ferrofluid rotary sealing system when ferrofluid is axially transported through its seals.

$$p_0 + p_{min} < p_l < p_0 + \sum_{j=1}^{n} \Delta p_j \tag{8}$$

where p_0 is the atmospheric pressure, p_{min} the minimum pressure, Δp_j the seal capacity of each seal ring j and n the number of seal rings in the system. It can be seen that if the number of seals increases, the operational range of sealing pressure p_l also increases.

Up to now the analysis has been performed assuming a non-rotating shaft. It is important to note that the sealing capacity decreases when the shaft speed increases. This also means that the operational range of the sealing system is different for static and dynamic sealing conditions. The refreshment rate of the seal system has to be sufficiently high in order to compensate for the degradation rate of the seal and thus to prevent seal failure. If the volume of the seal is known the specific replacement time of the ferrofluid seal can be calculated using the relation presented in equation (9).

$$R = \frac{\pi \cdot \left((r_s + h)^2 - r_s^2 \right) \cdot w_{seal}}{Q_{ff}} \tag{9}$$

where R is the time constant with which the seal is being replaced, r_s the shaft radius, h the seal gap height, w_{seal} the total seal width and Q_{ff} the ferrofluid supply rate. Without replenishment, the ferrofluid will degrade with a certain time constant, and will fail when the condition of the ferrofluid drops below a certain critical value. Now, with replenishment, the ferrofluid will still degrade but only until there is a balance between the addition of new ferrofluid and the degradation of ferrofluid in the seal, so the critical degradation value will never be reached.

2.6. Experimental test setup

The theory presented before is used to design and manufacture a ferrofluid rotary seal module and test setup in order to validate if the ferrofluid replenishment system improves and controls the service life of a ferrofluid rotary seal. An axially magnetised ring magnet (HKCM R15x08x06ZnPc-42SH, [35]) with a remanent magnetisation B_r of 1.28 T, also discussed in section 2.2, generates the magnetic field distribution inside of the ferrofluid sealing module. Corrosion of the magnet is prevented by its coating consisting of parylene and zinc. The shaft ($\varnothing = 7.8$ mm) is made of ferritic stainless steel (AINSI 430F), resulting in the magnetic field distribution presented in Fig. 2. The diametrical clearance between the ring magnet and the shaft is 200 μm and creates a seal gap of 100 μm. The ferrofluid used in the setup and experiments is Ferrotec EFH1 [36] and generates a theoretical sealing capacity of 96.2 kPa, which was calculated during the FEM analysis.

Fig. 6 presents an overview of the ferrofluid seal module that has been designed and manufactured. The ring magnet is contained in an assembly of four layers of transparent acrylic sheets that are bonded by transparent tape-sheet (3M 7955 MP). By using transparent structural material good visibility inside of the ferrofluid rotary seal is provided. Layer 1 functions as inner shield and creates a shielding channel that stabilises the liquid-ferrofluid interface. Acrylic sheet layer 2 contains a small milled channel of approximately 1 mm depth and width which is used for radial supply of ferrofluid in front of the first seal. The ring magnet is supported by layer 3 and this layer also contains a brass tube connector for the ferrofluid supply hose. Finally, layer 4 functions as outer shield and makes sure ferrofluid of the second seal is directed towards a low intensity region of the magnetic field. The magnetic field intensity plot of Fig. 3 showed that a layer thickness of 6 mm is sufficient in order to reach the full potential of the sealing capacity of the second ferrofluid seal.

Ferrofluid flows into the seal module via the inlet of layer 3 and enters through a hole in the supply channel of layer 2, which ends just before the first seal. Subsequently ferrofluid travels through the sealing channel to the ferrofluid outlet where it exits the system. Table 3 presents an overview of the width and function of the four layers of acrylic sheet.

In order to create the sealing environment the sealing module is mounted on a pressure chamber. Care is taken to ensure that only the shaft is ferro-magnetic, all other materials in the setup are non-magnetic. Fig. 7 presents a cross-sectional view of the test setup. The transparent acrylic cover end-plate provides good visibility inside of the pressure chamber. The total volume of the pressure chamber is approximately 58 ml. The liquid that is stored in the pressure chamber is pressurised by air through the pressure inlet. The shaft is supported by two pillow block ball bearings made of a zinc alloy. The ferrofluid supply hose is connected to the ferrofluid inlet of the seal module.

In order to perform consistent experiments it is important that the surface speed of the shaft is constant and therefore is velocity controlled. A 24 V brushless DC motor (Trinamic QBL4208-41-04-006) is connected to the shaft by a aluminum flexible motor coupling. The DC motor is supported by an acrylic structure and controlled using a single axis driver module (Trinamic TMCM-1640). A computer with software (Trinamic TMCL-IDE version 3.0) is connected to the driver module in order to provide instructions to the DC motor.

A rendering of the test setup is presented in Fig. 8. The pressure chamber is mounted to an acrylic baseplate by supports (6060T66 AlMgSi 0.5). The holes of these supports are slightly larger than the bolts used for mounting, enabling alignment of the seal module in both vertical and horizontal plane around the shaft. Additionally slots have been made in the acrylic support plate for alignment in the horizontal plane. The base consists of an aluminum breadboard (Thorlabs) with four

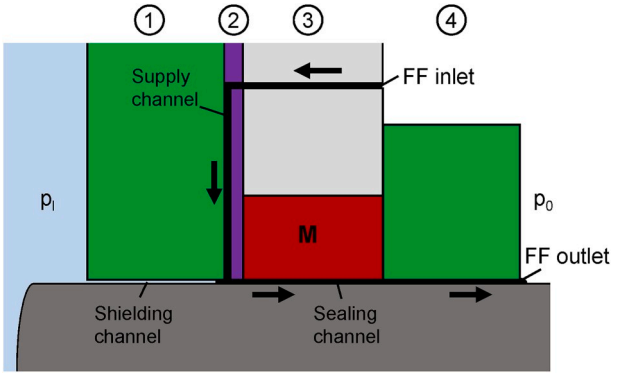

Fig. 6. Cross-sectional view of the seal module. The seal module consist of 4 different layers of transparent acrylic sheets.

Table 3
Overview of the transparent acrylic layers used in the sealing module. The layers are bonded by 127 μm transfer tape (3 M 7955 MP).

Layer	Width	Function
1	6 mm	Outer shield
2	2 mm	Supply channel
3	6 mm	Magnet support
4	6 mm	Inner shield

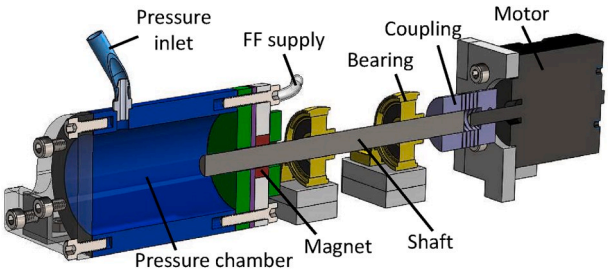

Fig. 7. Cross-section of the test setup. The seal module is mounted on a pressure chamber which creates the sealing environment. A DC motor drives the ferromagnetic shaft that is supported by two ball bearings.

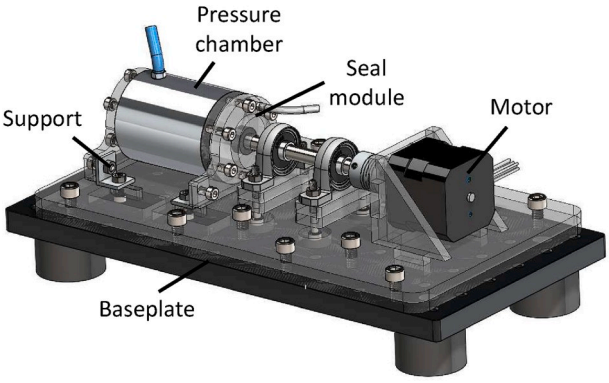

Fig. 8. Rendering of the experimental test setup. The setup is mounted on an aluminum breadboard base.

Sorborthane vibration isolaters (Thorlabs ⌀ 38.1 mm). Non magnetic stainless steel bolts are used throughout the system for mounting. The setup has been placed inside of an aluminum drip tray.

A global overview of the experimental test setup including supporting systems is presented in Fig. 9. The air pressure that is used in order to pressurise the pressure chamber is generated by a compressor and regulator. A needle valve is added for the manual fine-tuning of the pressure increase. In order to stabilise the pressure a buffer tank with a volume of 2 L is added. A ball valve is used to shut off the pressure of the pressure chamber after the desired sealing pressure is reached. Ferrofluid is rate controlled added to the system by the combination of a syringe pump (WPI SP100iZ) and a 3 ml syringe (HSW soft-ject). The device allows to set the rate and total volume of ferrofluid supply. The syringe and ferrofluid supply hose are connected by a Huer lock connection in order to make refill of the syringe convenient.

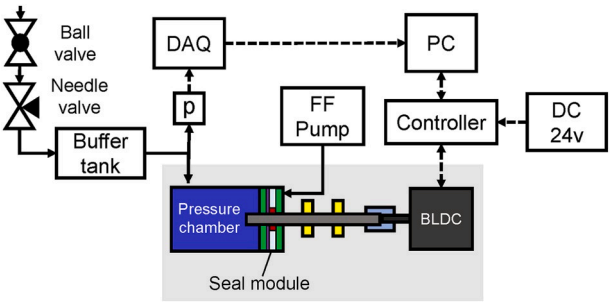

Fig. 9. Global overview of the experimental test setup and its supporting systems. Continuous arrows represent flows of air or ferrofluid, dotted arrows represent digital control signals.

The air inlet hose of the pressure chamber is split and connected to a monolithic silicon gauge pressure sensor (NXP MPX4250DP). The sensor measures the pressure inside of the pressure chamber (p_l) relative to the ambient air pressure (p_0). This means that the sealing capacity of the seal ($p_l - p_0$) is directly measured by the sensor. The sensor is connected to a 16 bit analog I/O device (NI USB-6211). Labview 2013 (version 13.0, 32 bit) has been used to live display the pressure inside of the pressure chamber and to store the sensor data that has been obtained during the experiments. The pressure is sampled at a frequency of 10 Hz.

2.7. Experimental procedure

2.7.1. Examination of sealing capacity

The first performance parameter of the ferrofluid sealing system that will be experimentally evaluated is its sealing capacity for a number of different static and dynamic sealing conditions. It is important that the exact moment of seal failure is accurately determined. That is why for the experiments evaluating the sealing capacity the buffer tank is removed. The sealing device is prepared for each sealing condition by first transporting ferrofluid through the sealing system. Once the sealing channel is completely filled with ferrofluid the supply is stopped and the seal is considered to be ready. During all experiments that have been performed the alignment between the seal module and shaft has not been changed.

First the static sealing capacity of the system is determined when it seals demineralised water. The sealing capacity is tested 5 times immediately after the test setup is prepared and 3 times 24 h after the setup is prepared. During this settling time of 24 h the seal is not pressurised, shaft speed is zero and the ferrofluid replenishment system is not active. These experiments are also conducted for air as sealed medium. The dynamic sealing capacity of the system when demineralised water is sealed is tested at five different shaft speeds, ranging from 500 to 2500 rpm.

In order to obtain the sealing capacity of the system during a certain sealing condition the pressure inside the pressure chamber will be increased until the seal bursts. The rate of pressure increase is manually controlled using the needle valve. The pressure of the pressure chamber is live monitored during the experiments. When the seal bursts during an experiment the needle and ball valve are closed.

2.7.2. Examination of service life

When the static and dynamic sealing capacity of the seal system are determined, the influence of the ferrofluid replenishment system on the service life of the seal can experimentally be examined. The service life of the seal system that seals demineralised water depends on shaft speed, sealing pressure and rate and duration of ferrofluid transport through the seal.

The pressure p_l of the demineralised water that is sealed is chosen to be at least higher than the sealing capacity of a single ferrofluid seal (48.1 kPa). By doing so, it is ensured that both ferrofluid seals have to contribute to the sealing capacity of the seal system when ferrofluid is transported through the seals. The upper bound of the sealing pressure is determined by the dynamic sealing capacity of the system at 500 rpm. The closer the sealing pressure p_l approaches this dynamic sealing capacity, the faster the seal will fail after the replenishment system is deactivated. The amount of time required to perform the experiments can be reduced this way. Within this range p_l is set at 55 kPa for the service life experiments (±90% of its dynamic sealing capacity at 500 rpm).

In order to examine the influence of the ferrofluid replenishment system on the service life of the seal, the ferrofluid replenishment system has been deactivated after various running times. These running times are 10, 30 and 60 min. The ferrofluid supply rate is set to 2 ml/h, which theoretically results in a replacement time constant of the ferrofluid in the system of approximately 1 min. The experiments are alternated in order to exclude coincidence. Five measurements per running time are performed.

3. Results and discussion

3.1. Static sealing capacity

The static sealing capacities of the seal that have been measured during the four different sealing conditions are listed in Table 4. The moments that the seal failed were very obvious, both from observation during the experiments as afterwards in the recorded pressure data. The average sealing capacity measured for water (75.9 kPa) and air (69.8 kPa) slightly differ.

The static sealing capacity that has been measured is lower than that was predicted by the analytical model and FEM analysis (96.2 kPa). Overestimation of the static sealing capacity could be due to wrong assumptions in the FEM analysis, analytical model or manufacturing errors in the test setup. Alignment of the shaft and the sealing module during the experiments was not perfectly concentric. Due to this misalignment the radial seal gap height h is larger than 100 μm at some locations in the seal system. This results in a lower magnetic field gradient at these weakest spots of the seal, thus lowering the sealing capacity of the system. Also the non uniformity of the coating of the ring magnet could introduce error in the height of the seal gap. Other authors have also reported that an increase in seal gap decreases the sealing capacity of the seal [37].

The FEM analysis did not account for the influence of ferrofluid on the magnetic field distribution in the system. Furthermore in the analytical model capillary effects have been neglected, which theoretically could lower the maximum pressure the sealed liquid can reach before the seal system fails. Other research also indicated that overestimation of the seal capacity of a ferrofluid seal could be due to capillary effects [6,38]. However, it has been shown that all these assumptions may only result in an acceptable small overestimation of the load capacity. As a consequence, this means manufacturing errors are probably the main reason that the sealing capacity is overestimated.

The average sealing capacity for water and air that was measured after the ferrofluid in the seal system had been allowed to settle for 24 h, 213 kPa and 156 kPa respectively, are significantly higher than the sealing capacity that is measured when it was tested immediately after preparation. A phenomenon that could attribute to this increase in seal capacity is the magnetic field gradient instability of the ferrofluid, which was presented in equation (6). The particles migrate through the fluid to locations that have a higher magnetic field intensity, which increases the effective magnetisation of the ferrofluid.

Also a difference in the sealing capacity for water and air after 24 h settling was observed. The sealing capacity measured after water has been sealed for 24 h (213 kPa) is larger than the sealing capacity when air is sealed for 24 h (156 kPa). This implies that the increase in static sealing capacity over time when water was sealed can not be attributed exclusively to the migration of particles to a higher magnetic field intensity.

The magnetic field intensity in the sealing gap and thus the sealing capacity of the seal can further be increased by adding pole pieces on both sides of the ring magnet [15]. Pole pieces consist of ferromagnetic material that concentrate the magnetic field in the seal gap. During this research the usage of pole-pieces has not been investigated.

Table 4
Average sealing capacity measured for four different static sealing conditions. Also the number of experiments per condition is listed.

Static condition	Mean $p_{c,s}$ [kPa]	#
Water	75.9	5
Air	69.8	5
Water (24 h)	213	3
Air (24 h)	156	3

3.2. Dynamic sealing capacity

Fig. 10 presents the dynamic sealing capacity of the ferrofluid rotary seal at different shaft speeds ranging from 0 till 2500 rpm. It can be seen that the sealing capacity of the seal drops when the shaft speed increases. The maximum pressure difference in [kPa] can be expressed as a function of the rotation speed in [rpm] by the exponential function $21.4 \cdot e^{-0.0019n} + 54.3$ fitted through the data with a coefficient of determination $R^2 = 0.94$.

The decrease in sealing capacity at higher shaft speeds shows similarities with other results found in literature. Szczech and Horak have proposed a mathematical model that can be used to predict the dynamic sealing capacity of a seal [13]. However, the dynamic sealing capacity that is calculated using this model predicts a faster decrease in sealing capacity at high speeds than is measured. The setup that they have used in order to derive their mathematical model did not contain a shield. This could suggest that a shield can also be used to improve dynamic sealing capacity. Further research is required in order to validate this.

It is not fully understood why the sealing capacity drops when the shaft speed increases. It is possible that higher inertial and viscous effects result into a faster destabilisation of the ferrofluid flow inside of the seal, which affects the sealing capacity of the system. Also some authors consider the Kelvin-Helmholtz instability that was mentioned in section 2.4 as the main reason for the dynamic sealing capacity to decrease [13, 18]. However, since the test setup contains a shield, the relative velocity between the water that is sealed and the ferrofluid of the seal is minimal. Furthermore it is not evident how the pressure of the liquid that is sealed is related to the stability of the interface between the ferrofluid and the liquid.

3.3. Service life

Fig. 11 presents the results of the service life experiments on the ferrofluid rotary seal with replenishment system. In the graph 15 measurements of the water pressure inside of the pressure chamber are presented. All measurements start at a water pressure p_l of 55 kPa and for each of the measurements a sudden drop in pressure after a period of time can be seen. This drop indicates the moment the seal has failed and has started to leak water through the sealing channel. After that, when

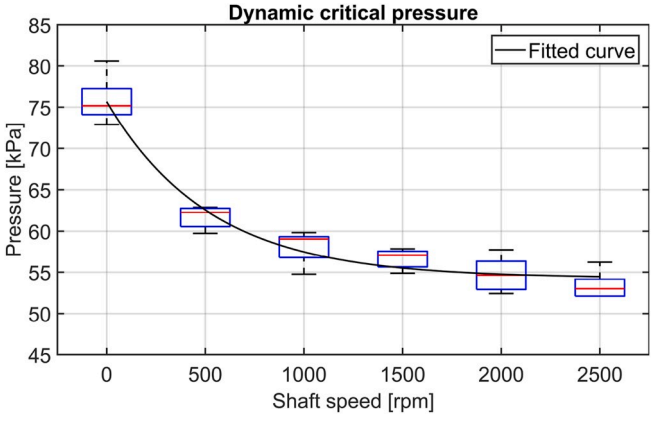

Fig. 10. Boxplot of the measured dynamic sealing capacity of the seal system at different shaft speeds. The fitted line through the data is $21.4 \cdot e^{-0.0019n} + 54.3$.

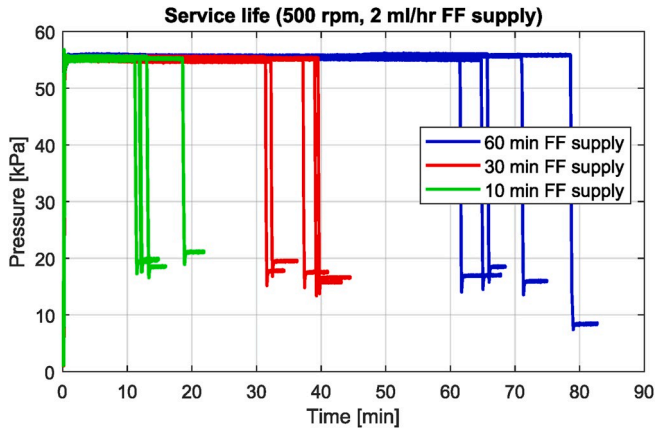

Fig. 11. Service life of the ferrofluid rotary seal when the ferrofluid replenishment system is deactivated after 10, 30 or 60 min. Water pressurised at 55 kPa is sealed at a shaft speed of 500 rpm. The ferrofluid supply rate is 2 ml/h.

the pressure had dropped sufficiently the ferrofluid that has remained on the ring magnet is able to form a new seal and the pressure inside of the container is again stabilised. It can be observed that during most of the measurements a new seal was formed at a pressure slightly below 20 kPa. After the seal stabilised the measurements were stopped.

During the measurements presented in Fig. 11 ferrofluid transport through the seals of 2 ml/h was stopped after 10, 30 or 60 min respectively. When the ferrofluid supply was stopped after 10 min the seal failed within 20 min. If the ferrofluid supply was stopped after 30 min, service life of the seal increased to approximately 30–40 min. Finally, if ferrofluid supply was only stopped after 60 min, service life ranged from approximately 60 till 80 min. The measurement presented in Fig. 11 show that the ferrofluid rotary seal did not fail while the replenishment system was active.

Because the seal module is transparent and easily accessible it could visually be confirmed that ferrofluid is transported through the seal to the outlet of the seal system while the replenishment system was active. Due to gravity the ferrofluid at the output of the seal leaked along the shield on the base-plate.

The measurements of the pressure in Fig. 11 show that the moment the seal fails can be controlled by the ferrofluid replenishment system. The ferrofluid supply rate of 2 ml/h results in a specific replacement time of approximately 1 min. The sealing pressure of 55 kPa during the service life experiments is higher than the sealing capacity of a single ferrofluid seal. This means that at the same time that ferrofluid was transported from one seal to another, both seals still were able to maintain their sealing capacity.

It can be seen that the original service life of the seal without active ferrofluid replenishment system is short and ranges from a few minutes to 20 min. This short service life of the seal without ferrofluid replenishment was expected, since the seal was operating at 90% of its dynamic sealing capacity. It also has been found in literature that service life becomes shorter when the sealing pressure becomes higher [14]. The ferrofluid supply rate that is required in order to prevent failure of the ferrofluid seal is dependent on the degradation rate of the seal. It is expected that the required supply rate decreases when the original service life of the seal is higher at lower sealing pressures.

During ferrofluid transport through the seal no water was observed at the ferrofluid outlet of the seal. However, the composition and properties of the ferrofluid leaving the seal and of the water in the pressure chamber were not investigated in this research and therefore the presence or absence of water in the ferrofluid outflow cannot be confirmed.

4. Conclusion

In this research it is demonstrated that the service life of a ferrofluid rotary seal that dynamically seals pressurised water successfully can be improved and controlled by implementing a ferrofluid replenishment system in its design. Degradation of the ferrofluid in the seal ring over time decreases its sealing capacity, which results in seal failure when the sealing capacity becomes lower than the operational sealing pressure. If the ferrofluid seals in the system are completely replaced at a sufficient rate, service life of the seal theoretically will be unlimited.

The increase in static sealing capacity over time that was observed during the experiments could partially be attributed to the migration of particles through the carrier liquid towards higher magnetic field intensities.

Overall, it is believed that the implementation of a ferrofluid replenishment system in ferrofluid rotary seals will pave the way for the development of a new rotary sealing technology for liquids promising low friction in combination with infinite lifetime and zero leakage.

Declaration of competing interest

The authors declare that they have no known competing financial interests or personal relationships that could have appeared to influence the work reported in this paper.

CRediT authorship contribution statement

Karoen van der Wal: Investigation. **Ron A.J. van Ostayen:** Supervision. **Stefan G.E. Lampaert:** Investigation, Supervision.

Acknowledgement

This research was funded by the Dutch TKI Maritime Funding Program.

References

[1] S. Papell, “Low viscosity magnetic fluid obtained by the colloidal suspension of magnetic particles: Us, 3215572.”.
[2] Rosensweig RE. Ferrohydrodynamics. Courier Corporation; 2013.
[3] Rosensweig R. Directions in ferrohydrodynamics. J Appl Phys 1985;57(8):4259–64.
[4] Scherer C, Figueiredo Neto AM. Ferrofluids: properties and applications. Braz J Phys 2005;35(3A):718–27.
[5] Bailey R. Lesser known applications of ferrofluids. J Magn Magn Mater 1983;39(1–2):178–82.
[6] Lampaert S, Spronck J, van Ostayen R. Load and stiffness of a planar ferrofluid pocket bearing. Proc IME J J Eng Tribol 2018;232(1):14–25.
[7] Lampaert S, Fellinger B, Spronck J, Van Ostayen R. In-plane friction behaviour of a ferrofluid bearing. Precis Eng 2018;54:163–70.
[8] Baart P, Lugt P, Prakash B. Review of the lubrication, sealing, and pumping mechanisms in oil-and grease-lubricated radial lip seals. In: Proceedings of the institution of mechanical engineers. Part J: journal of engineering tribology, vol. 223; 2009. p. 347–58.
[9] Szydlo Z, Ochoński W, Zachara B. Experiments on magnetic fluid rotary seals operating under vacuum conditions. Tribotest 2005;11(4):345–54.
[10] Anton I, De Sabata I, Vekas L, Potencz I, Suciu E. Magnetic fluid seals: some design problems and applications. J Magn Magn Mater 1987;65(2–3):379–81.
[11] Raj K, Stahl P, Bottenberg W. Magnetic fluid seals for special applications. ASLE Trans 1980;23(4):422–30.
[12] Raj K, Moskowitz B, Casciari R. Advances in ferrofluid technology. J Magn Magn Mater 1995;149(1–2):174–80.
[13] Szczech M, Horak W. Tightness testing of rotary ferromagnetic fluid seal working in water environment. Ind Lubric Tribol 2015;67(5):455–9.
[14] Matuszewski L, Szydlo Z. Life tests of a rotary single-stage magnetic-fluid seal for shipbuilding applications. Pol Marit Res 2011;18(2):51–9.
[15] Liu T, Cheng Y, Yang Z. Design optimization of seal structure for sealing liquid by magnetic fluids. J Magn Magn Mater 2005;289:411–4.
[16] Mitamura Y, Sekine K, Asakawa M, Yozu R, Kawada S, Okamoto E. A durable, non power consumptive, simple seal for rotary blood pumps. Am Soc Artif Intern Organs J 2001;47(4):392–6.
[17] Heinz K, Müller B, Nau S. Fluid sealing technology principles and applications. 1998.
[18] Kurfess J, Müller H. Sealing liquids with magnetic liquids. J Magn Magn Mater 1990;85(1–3):246–52.

[19] Mitamura Y, Yano T, Nakamura W, Okamoto E. A magnetic fluid seal for rotary blood pumps: behaviors of magnetic fluids in a magnetic fluid seal. Bio Med Mater Eng 2013;23(1–2):63–74.
[20] Sekine K, Mitamura Y, Murabayashi S, Nishimura I, Yozu R, Kim D-W. Development of a magnetic fluid shaft seal for an axial-flow blood pump. Artif Organs 2003;27(10):892–6.
[21] Mitamura Y, Takahashi S, Amari S, Okamoto E, Murabayashi S, Nishimura I. A magnetic fluid seal for rotary blood pumps: long-term performance in liquid. Phys Procedia 2010;9:229–33.
[22] Mitamura Y, Arioka S, Sakota D, Sekine K, Azegami M. Application of a magnetic fluid seal to rotary blood pumps. J Phys Condens Matter 2008;20(20):204145.
[23] Wang H, Li D, Wang S, He X, Zhen S. Effect of seal gap on the seal life when sealing liquids with magnetic fluid. Rev Fac Ingen 2016;31(12):83–8.
[24] Jarmo V, Matti E, Raimo P. Sealing of liquids with magnetic fluid seals. In: In 6th nordic symposium on tribology; 1994. p. 697–702. Szwecja.
[25] Matuszewski L, Szydło Z. The application of magnetic fluids in sealing nodes designed for operation in difficult conditions and in machines used in sea environment. Pol Marit Res 2008;15(3):49–58.
[26] Szydło Z, Matuszewski L. Experimental research on effectiveness of the magnetic fluid seals for rotary shafts working in water. Pol Marit Res 2007;vol. 14:53–8.
[27] Mitamura Y, Fujiyoshi M, Yoshida T, Yozu R, Okamoto E, Tanaka T, Kawada S. A ferrofluidic seal specially designed for rotary blood pumps. Artif Organs 1996;20 (5):497–502.
[28] Rosensweig R. Ferrohydrodynamics. Dover Publications; 1998. 5.
[29] Perez-Castillejos R, Plaza J, Esteve J, Losantos P, Acero M, Cané C, Serra-Mestres F. The use of ferrofluids in micromechanics. Sensor Actuator Phys 2000;84(1–2): 176–80.
[30] Polevikov V, Tobiska L. Influence of diffusion of magnetic particles on stability of a static magnetic fluid seal under the action of external pressure drop. Commun Nonlinear Sci Numer Simulat 2011;16(10):4021–7.
[31] Hujun Wang DL. Effect of the seal gap on the seal life when sealing liquids with magnetic fluid. Revista de la Facultad de Ingenieria U.C.V. 2016;31(12):83–8.
[32] Potma O. "Designs for rotary shaft fluid seals in an aqueous environment using ferrofluid," Master's thesis. Delft University of Technology; 2017.
[33] Potma O, Lampaert S, van Ostayen R. Method for transport of ferrofluid in a liquid contactless rotational seal. In: In Conference report: 17th EDF–Pprime workshop; 2018. p. 10.
[34] Szczch M. Experimental study on the pressure distribution mechanism among stages of the magnetic fluid seal. IEEE Trans Magn 2018;54(6):1–7.
[35] HKCM Engineering e. K. Magnet-ring R15x08x06ZnPc-42SH. Datasheet; 2018. p. 5.
[36] Ferrotec Corporation, Ferrofluid EFH1. Safety datasheet. 5. 2014.
[37] Li DC, Zhang HN, Zhang ZL. Study on magnetic fluid static seal of large gap. In key engineering materials, vol. 512. Trans Tech Publ; 2012. p. 1448–54.
[38] Boots A, Krijgsman L, de Ruiter B, Lampaert S, Spronck J. Increasing the load capacity of planar ferrofluid bearings by the addition of ferromagnetic material. Tribol Int 2019;129:46–54.